nal gain in the individual QDs is high and that the captures and thermalization of the injected carriers must be efficient because the QD coverage is at most 50% and, because of the inhomogeneous broadening of 60 meV, only a small fraction (estimated to be 5%) of the QDs can emit at the lasing energy. The threshold current density of the QD laser changed little between 4 and 77 K but increased quite rapidly above 80 K. This decrease in the QD laser efficiency at higher temperature is most likely due to a nonoptimized laser design. For example, thermal quenching of the PL in self-assembled QDs is caused by thermionic emission of the carriers above the confining barriers (*14*). Therefore, an increase in the confinement of the injected carriers that have thermalized in the QDs and in the separate confinement regions of the structures would increase the maximum operating temperature.

The inhomogenous energy broadening associated with the size, composition, and strain variations typical for self-assembled QDs is not too large to destroy the optical gain. With a large enough density of self-assembled QDs, the higher gain associated with the 0D density of states compensates for the unused QDs having an emission energy different from the stimulated emission energy that is supported by the lasing cavity. The 60-meV broadening might therefore offer a wider range of optical gain, which could be exploited in the case of a tunable laser diode structure. Such a uniformity requirement is easily achieved with the spontaneous islanding. However, because of the atomic dimensions involved, it is also unlikely that the present uniformity will be much exceeded. It would be difficult to achieve much higher densities of monochromatic QDs to further improve the conversion efficiency of single-layer QD lasers. However, the prospect of increasing the total number of active QDs by exploiting strain-induced self-organizing mechanisms to grow a stack of several layers of uniform QDs appears to be a promising approach (*19–22*).

REFERENCES AND NOTES

1. D. Mehuys and D. Evans, *Laser Focus World* **31**, 117 (1995); J. Hecht, *ibid.* **29**, 83 (1993); A. Strass, *ibid.* **30**, 79 (1994).
2. D. Leonard, M. Krishnamurthy, S. Fafard, J. M. Merz, P. M. Petroff, *J. Vac. Sci. Technol. B* **12**, 1063 (1994); D. Leonard, K. Pond, P. M. Petroff, *Phys. Rev. B* **50**, 11687 (1994); D. Leonard *et al.*, *J. Vac. Sci. Technol. B* **12**, 2516 (1994).
3. J. M. Moison *et al.*, *Appl. Phys. Lett.* **64**, 196 (1994).
4. S. Fafard, R. Leon, D. Leonard, J. L. Merz, P. M. Petroff, *Phys. Rev. B* **50**, 8086 (1994); *Superlattices Microstruct.* **16**, 303 (1994); S. Fafard, D. Leonard, J. L. Merz, P. M. Petroff, *Appl. Phys. Lett.* **65**, 1388 (1994).
5. J.-Y. Marzin, J.-M. Gérard, A. Izraël, D. Barrier, G. Bastard, *Phys. Rev. Lett.* **73**, 716 (1994).
6. H. Drexler, D. Leonard, W. Hansen, J. P. Kottaus, P. M. Petroff, *ibid.*, p. 2252.
7. M. Grundmann *et al.*, *ibid.* **74**, 4043 (1995); M. Grundmann *et al.*, *Phys. Status Solidi* **188**, 249 (1995).
8. S. Fafard, R. Leon, D. Leonard, J. L. Merz, P. M. Petroff, *Phys. Rev. B* **52**, 5752 (1995); S. Raymond *et al.*, *ibid.*, p. 17238.
9. R. Nötzel *et al.*, *Appl. Phys. Lett.* **66**, 2525 (1995).
10. R. Leon, P. M. Petroff, D. Leonard, S. Fafard, *Science* **267**, 1966 (1995); R. Leon, S. Fafard, D. Leonard, J. L. Merz, P. M. Petroff, *Appl. Phys. Lett.* **67**, 521 (1995).
11. K. Imamura *et al.*, *Jpn. J. Appl. Phys. A* **11**, L1445 (1995).
12. S. Fafard, Z. Wasilewski, J. McCaffrey, S. Raymond, S. Charbonneau, *Appl. Phys. Lett.* **68**, 991 (1996).
13. M. Grundmann *et al.*, *ibid.*, p. 979.
14. S. Fafard *et al.*, *Surface Sci.* **361–362**, 778 (1996).
15. R. Heitz *et al.*, *Appl. Phys. Lett.* **68**, 361 (1996).
16. S. Raymond *et al.*, *Phys. Rev. B* **54**, 11548 (1996).
17. U. Bockelmann and G. Bastard, *ibid.* **42**, 8947 (1990); U. Bockelmann and T. Egeler, *ibid.* **46**, 15574 (1992); U. Bockelmann, *ibid.* **48**, 17637 (1993).
18. K. Kamath, P. Bhattacharya, T. Sosnowski, T. Norris, J. Phillips, *Electron. Lett.* **32**, 1374 (1996).
19. H. Shoji *et al.*, *IEEE Photonics Technol. Lett.* **7**, 1385 (1995); H. Shoji *et al.*, *Jpn. J. Appl. Phys. II, Lett.* **35**, L903 (1996).
20. Z. I. Alferov *et al.*, *Semiconductors* **30**, 194 (1996); O. G. Schmidt *et al.*, *Electron. Lett.* **32**, 1302 (1996). N. Kirstaedter *et al.*, *ibid.* **30**, 1416 (1994).
21. Q. Xie, A. Kalburge, P. Chen, A. Madhukar, *IEEE Photonics Technol. Lett.* **8**, 965 (1996).
22. J. Tersoff, C. Teichert, M. G. Lagally, *Phys. Rev. Lett.* **76**, 1675 (1996).

23. We thank Z. Wasilewski, P. Hawrylak, P. T. Coleridge, and P. Corkum for helpful discussions. The technical assistance of J. Stapledon, P. Chow-Chong, P. Marshall, and A. Golsham is also acknowledged.

1 August 1996; accepted 2 October 1996

Chemiluminescence in the Agglomeration of Metal Clusters

L. König, I. Rabin, W. Schulze, G. Ertl*

The agglomeration of copper or silver atoms in a matrix of noble gas atoms to form small clusters may be accompanied by the emission of visible light. Spectral analysis reveals the intermediate formation of electronically excited atoms and dimers as the source of the chemiluminescence. A mechanism is proposed, according to which the gain in binding energy upon cluster formation may even lead to the ejection of excited fragments as a result of unstable intermediate configurations. A similar concept was introduced in the field of nuclear reactions by Niels Bohr 60 years ago.

Exothermic chemical reactions may be accompanied by chemiluminescence. In these reactions, the released energy is not adiabatically damped into the heat bath of the surrounding medium but rather is stored in an excited state of the product; decay from this excited state to the ground state is associated with light emission. In the course of our studies into the formation of metal clusters, we discovered, under specific conditions, the emission of visible light, as well as evidence for the production of electronically excited atoms and dimers.

The effect was discovered in an experimental arrangement comprising a cluster source based on the gas aggregation technique. Metal atoms thermally evaporated from a Knudsen cell are transported by a stream of noble gas into a nucleation zone, where cooling of the gas stream by the cold walls leads to homogeneous nucleation and growth of clusters. The cluster size distribution can be varied from 2 (dimers) to about 10^4 atoms per cluster (*1*) by changing the experimental conditions. The clusters leaving the source together with large quantities of the carrier gas can be subjected to various experiments and are eventually trapped at the walls of a cryopump cooled by liquid He, where a cluster-doped noble gas matrix is formed at high deposition rates.

In the course of such experiments with small clusters of Cu, Ag, or Au, the emission of light from the growing layers was visually observed under specific conditions. The intensity depended on matrix temperature and metal concentration.

To study these effects in detail, we modified the cluster source to allow the formation of matrices on a quartz window of a cryostat with an unusually high gas deposition rate (about 10^{18} atoms s^{-1} cm^{-2}) and with a gas-to-metal ratio exceeding 5000. The growth rate of the matrix was about 1 cm $hour^{-1}$, so that rather thick layers were formed. As a consequence, the gas loss due to re-evaporation was negligible during warm-up experiments, even at 50 K. Under these operating conditions, mainly atoms and dimers are produced by the cluster source. The emitted light was analyzed by a monochromator coupled to a CCD (charge-coupled device) detector system. Possible influences by spurious effects were carefully checked: We eliminated the possibility of energy supply by electrons or ions from the

---

Fritz-Haber-Institut der Max-Planck-Gesellschaft, Faradayweg 4-6 (Dahlem), D-14195 Berlin, Germany.

*To whom correspondence should be addressed. E-mail: ertl@fhi-berlin.mpg.de

cluster source by applying deflection electric fields, and chemical reaction with impurities (for example, oxidation) was tested by intentional admixture of air, which was found not to affect the observation of chemiluminescence.

The temperature of the noble gas matrix (as determined by the substrate temperature) had a significant influence. At higher temperatures, luminescence was observed continuously during deposition, whereas the intensity was much weaker at lower temperatures; however, in the latter case subsequent warming then initiated light emission (Fig. 1). These findings indicate that the observed light emission is a consequence of the agglomeration of clusters inside the noble gas matrix; this process requires the temperature to be high enough to warrant sufficient mobility. The shape of the curve suggests that the mobility of the clusters depends on their size.

Coalescing Cu clusters emitted light in two characteristic spectral regions (Fig. 2). Variation of the noble gas had only a minor influence on the spectral characteristics; however, Ne presented the less perturbing medium, and therefore, vibrationally resolved spectra, for example, of dimers can be easily obtained in a Ne matrix. The two bands between 400 and 500 nm exhibit clearly resolved vibrational structure (Fig. 2A) and were identified as B → X and A → X transitions of electronically excited Cu dimers on the basis of agreement with the respective fluorescence spectra (*2*). The sharp peaks on the broad emission between 700 and 900 nm (Fig. 2B) are attributed to $^2D \rightarrow {}^2S$ transitions of Cu atoms in Ar, again based on comparison with respective fluorescence spectra (*3*). The broad emission is attributed to Cu_n clusters ($n \geq 3$). Qualitatively analogous observations were made with Ag clusters.

This is by no means the first observation of the formation of electronically excited particles in a chemical reaction. For example, vibrationally resolved chemiluminescence of the CaF* species in the reaction $Ca + F_2 \rightarrow CaF^* + F$ has been observed (*4*). However, in the present system, the electronic excitation is the consequence of the interaction between ensembles of equal atoms, rather than of different elemental species as with the quoted system. In addition, the observed effects cannot be attributed to the formation of single chemical bonds between atoms. We now outline the proposed mechanism for the case of Ag, for which reliable theoretical data for the energetics of cluster formation are available (*5*).

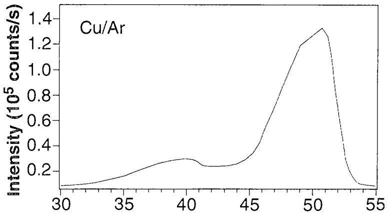

Fig. 1. Intensity of the light (of wavelength 250 to 1000 nm) emitted during the warm-up of a Cu-doped Ar matrix prepared at 30 K.

As with Cu, the agglomeration of Ag clusters was accompanied by, among other things, light emission centered at 476 nm, which is attributed to the decay of Ag_2^*, corresponding to an excitation energy of 2.6 eV (very weak emission was recorded at photon energies of up to 5 eV, and additional strong emissions were detected at 619 and 970 nm). The binding energy of Ag_2 amounts, however, to only 1.6 eV (*5*), and hence, the recombination of two Ag atoms cannot account for the observed effect. We conclude that the coagulation of multiatomic ensembles causes the ejection of smaller, excited particles (say M_2 or M) from an electronically excited intermediate state

$$M_n + M_m \rightarrow M^*_{m+n} \rightarrow M_{m+n-1} + M^* \rightarrow M_{m+n-1} + M + h\nu \quad (1a)$$

$$M_n + M_m \rightarrow M^*_{m+n} \rightarrow M_{m+n-2} + M_2^* \rightarrow M_{m+n-2} + M_2 + h\nu \quad (1b)$$

where $h\nu$ is the energy of the emitted photon. For example, according to theoretical calculations (*5*), the reaction $Ag_5 + Ag_3 \rightarrow Ag_8$ is associated with an energy gain of 5.2 eV, which could lead to the formation of an electronically excited Ag_8^* species from which an excited Ag* could be ejected. Dissociation of Ag_8 from the ground state into Ag_7 + Ag would require an energy of 2.5 eV, so that 2.7 eV of excitation energy would still be stored in the Ag*, but corresponding data for excited states are not yet available and might be quite different. Characterization of the matrix-isolated particles at varying conditions (of metal concentration and temperature) by means of ultraviolet absorption spectroscopy revealed that chemiluminescence is never observed if only single atoms recombine; it requires the presence of larger aggregates, which supports the proposed mechanism (*6*).

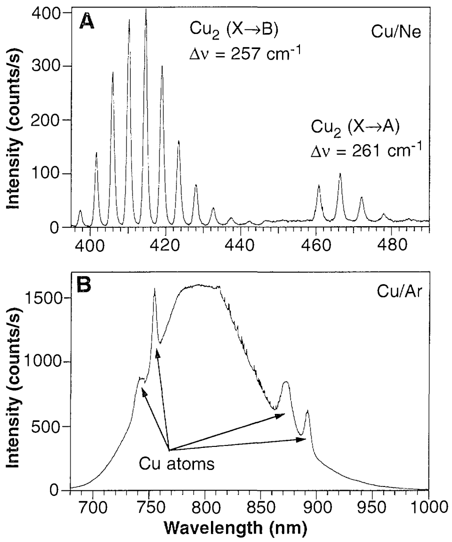

Fig. 2. Spectral distributions of the chemiluminescence during the agglomeration of Cu clusters in noble gas matrices: (**A**) Cu dimer emission (in Ne); (**B**) Cu atom $^2D \rightarrow {}^2S$ emissions (sharp lines) and a broad emission from an unknown Cu_n cluster with $n \geq 3$ (in Ar). In (A), $\Delta\nu$ is the vibrational splitting between two neighboring peaks.

The electronically excited intermediate state formed after the coagulation of multiatomic ensembles can also decay directly

$$M_n + M_m \rightarrow M^*_{m+n} \rightarrow M_{m+n} + h\nu \quad (2)$$

The broad unassigned band in Fig. 2B may be the result of such a process.

The proposed reaction scheme is analogous to the concept developed by Bohr (*7*) for nuclear collision reactions. Such processes may be rationalized in terms of the formation of a "compound" nucleus in which the excess energy is shared between all constituents, followed by subsequent disintegration. For the latter process, a statistical theory was developed by Weisskopf (*8*), and this theory has recently also been adopted to model the fragmentation of hot atomic metal clusters (*9*). It has to be kept in mind, however, that this latter work treated only evaporation from the electronic ground state of the cluster. The ejection of ground-state atoms and dimers has also been observed experimentally in collision-induced fragmentation reactions of metal cluster ions (*10*) in which the necessary energy was provided by the kinetic energy of collisions. By contrast, in the present case it is the gain in binding energy associated with the agglomeration of clusters that causes either ejection of fragments in electronically excited states or a direct decay of the intermediate state.

In the course of the present study, we performed time-resolved fluorescence measurements by applying synchrotron radiation from the Berlin Electron Storage Ring for Synchrotron Radiation (single-bunch mode) source. The lifetime of, for example, photostimulated Ag_2^* giving rise to emission at 476 nm in an Ar matrix was determined to be 4.6×10^{-9} s, which compares well with literature data (*11*); for Ag_3^*, a lifetime of 12.7×10^{-9} s was measured. This lifetime is likely to be long enough compared with the time for disintegration of the excited "compound" clusters to explain why the excess energy is not completely quenched in radiationless processes but may manifest itself in light emission from the separated fragments.

REFERENCES

1. F. Frank, W. Schulze, B. Tesche, J. Urban, B. Winter, *Surf. Sci.* **156**, 90 (1985).
2. J. L. Gole, J. H. English, V. E. Bondebey, *J. Phys. Chem.* **86**, 2560 (1982); D. M. Kolb, H. H. Rotermund, W. Schrittenlacher, W. Schroeder, *J. Chem. Phys.* **80**, 695 (1984).
3. W. Schrittenlacher and D. M. Kolb, *Ber. Bunsenges. Phys. Chem.* **88**, 492 (1984).
4. M. G. Prisant, C. T. Rettner, R. N. Zare, *J. Chem. Phys.* **81**, 2699 (1984).
5. V. Bonacic-Koutecky, L. Cespiva, P. Fantucci, J. Koutecky, *Z. Phys. D* **26**, 287 (1993).
6. L. König, I. Rabin, W. Schulze, G. Ertl, in preparation.
7. N. Bohr, *Nature* **137**, 344 (1936).
8. V. Weisskopf, *Phys. Rev.* **52**, 295 (1937).
9. P. A. Hervieux and D. H. E. Gross, *Z. Phys. D* **33**, 295 (1995).
10. S. Becker *et al.*, *ibid.* **30**, 341 (1994); C. Bréchignac *et al.*, *Phys. Rev. Lett.* **72**, 1636 (1994).
11. T. Hebert *et al.*, *J. Chem. Phys.* **91**, 1417 (1989).

5 August 1996; accepted 22 October 1996

Glacial to Interglacial Fluctuations in Productivity in the Equatorial Pacific as Indicated by Marine Barite

A. Paytan, M. Kastner, F. P. Chavez

An empirical correlation between marine barite ($BaSO_4$) accumulation rate in core-top sediment samples from two equatorial Pacific transects (at 140°W and 110°W) and the estimated primary productivity of the overlying water column were used to evaluate glacial to interglacial changes in productivity. Fluctuations in barite accumulation rates down-core indicate that during glacial periods of the past 450,000 years, the productivity in the central and eastern equatorial Pacific was about two times that during intervening interglacial periods. This result is consistent with other evidence that productivity was high in the eastern and central equatorial Pacific during the last glacial.

Ocean productivity influences organic carbon supply to the sediment and its burial efficiency, affecting the partitioning of CO_2 between the ocean and atmosphere, and thus climate (*1–3*). Large glacial to interglacial fluctuations in atmospheric CO_2 concentrations have been observed in ice cores and related to variations in ocean productivity (*4*, *5*). In order to discern the coupling between ocean circulation, productivity, and climate, it is important to be able to estimate past ocean productivity and thus to reconstruct its history from the record of marine sediments (*6*).

We use barite accumulation rate (AR_{BaSO4}) in sediments to reconstruct changes in productivity in the equatorial Pacific for the past 450,000 years and to relate these fluctuations to the climate record. The equatorial Pacific region is emphasized because upwelling of CO_2-rich waters in this region provides the largest natural source of CO_2 to the atmosphere (*7*, *8*).

Barite is a suitable proxy for oceanic productivity because biogenic Ba in sediment traps (*9*, *10*) and marine barite in deep-sea sediments (*11–14*) correlate well with the overlying productivity, and because of its low solubility barite tends to be preserved in pelagic sediments (*9*). Moreover, barite is not affected by burial diagenesis in oxic sediments (*15*). The exact mechanism of barite formation is as yet unknown, but there are indications that in the ocean it precipitates in micro-environments containing decaying organic matter, acantharian shells, and other biogenic remains (*16–18*). Earlier studies have estimated paleoproductivity from total Ba concentration in sediments or in sediment traps (*9*, *19–22*). For this, however, various assumptions and corrections are required because Ba is a component of sediment phases not directly related to biogenic productivity, such as windblown silicates and Fe-Mn oxyhydroxides (*9*). We measured, instead, only the concentration of barite grains, the dominant Ba-bearing phase related to biological productivity (*9–11*, *23*).

We separated barite from equatorial Pacific sediments using a sequential leaching method (*18*); yields were between 90 to 95% and the reproducibility was within ±5%. The cores selected are from two transects across a region of the equatorial Pacific (12°S to 11°N at 110°W and 140°W) where productivity in the overlying water columns varies greatly (*8*). We determined AR_{BaSO4} from weight percent barite, sedimentation rates, and sediment dry bulk densities (*24*). Gross primary productivity estimates were compiled from measurements made over the past 12 years (*25–28*). At both transects, the maxima in AR_{BaSO4} and productivity were centered at the equator (Fig. 1), at the 110°W transect however, this zone is somewhat wider. Other productivity indicators [abundance of $CaCO_3$ and organic carbon (*29*) and Al/Ti (*30*), Pa/Th, and Be/Th (*31*) ratios] show similar distributions. A positive association between AR_{BaSO4} and the mean primary productivity in the overlying water column is obtained from the data in Fig. 1 and from a few other equatorial Pacific core tops (Fig. 2). The empirical relation obtained is a result of both productivity (barite rain rate) and sedimentary processes. The positive intercept of the linear fit indicates that in low-productivity areas the regeneration of barite in the sediment is equal to the rain rate, resulting in zero barite accumulation. Assuming that the relation between productivity and sediment accumulation has not differed greatly and that the same processes governing barite accumulation (supply from the water column and formation at the sediment water interface) and preservation (dissolution in the sediment) have persisted in the past, we can use this empirical relation to estimate past productivity in this area.

We computed AR_{BaSO4} in two cores

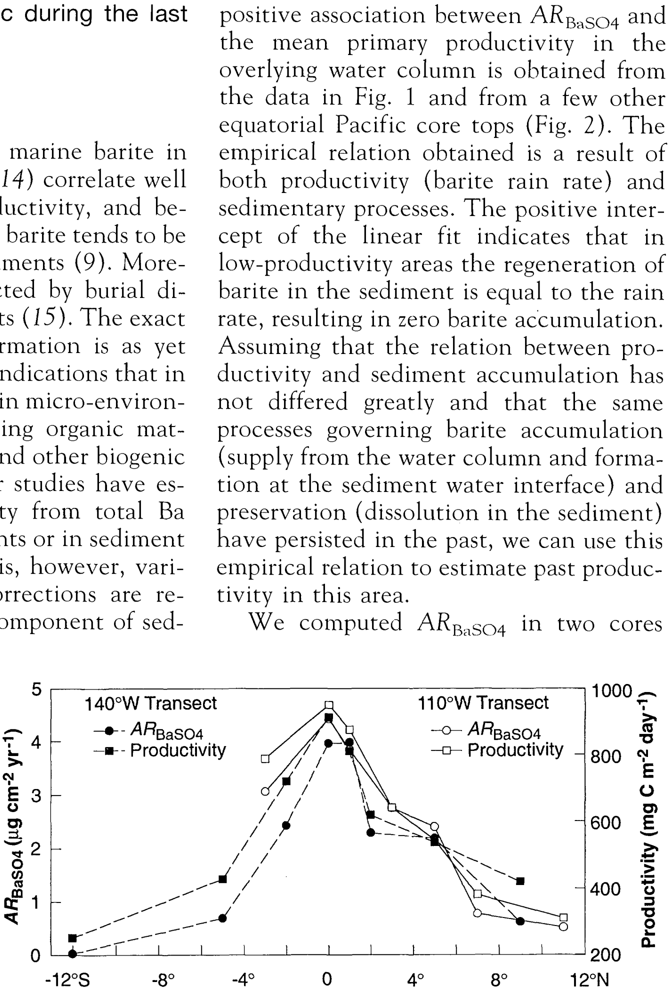

Fig. 1. Barite accumulation rates (AR_{BaSO4}) (circles) and primary productivity (squares) in equatorial Pacific core-top sediments (0 to 5 cm) along the TT013 transect at 140°W (full symbols) and VNTR01 transect at 110°W (open symbols).

A. Paytan and M. Kastner, Scripps Institution of Oceanography, University of California San Diego, La Jolla, CA 92093-0212, USA. E-mail: apaytan@ucsd.edu
F. P. Chavez, MBARI, Post Office Box 628, 7700 Sandholdt Road, Moss Landing, CA 95039-0628, USA.